Advances in Nano Research, *Vol. 2, No. 4 (2014) 179-186*
DOI: http://dx.doi.org/10.12989/anr.2014.2.4.179

Effects of post anneal for the INZO films prepared by ultrasonic spray pyrolysis

Wen-How Lan[1], Yue-Lin Li[1], Yu-Chieh Chung[1], Cheng-Chang Yu[2], Yi-Chun Chou[1], Yi-Da Wu[1], Kai-Feng Huang[2] and Lung-Chien Chen[*3]

[1]*Department of Electrical Engineering, National University of Kaohsiung, Nan-Tzu 811, Kaohsiung, Taiwan*
[2]*Department of Electrophysics, National Chiao Tung University, Hsinchu 300, Taiwan*
[3]*Department of Electro-optical Engineering, National Taipei University of Technology, Taipei 106, Taiwan*

(Received August 5, 2014, Revised January 13, 2015, Accepted January 14, 2015)

Abstract. Indium-nitrogen co-doped zinc oxide thin films (INZO) were prepared on glass substrates in the atmosphere by ultrasonic spray pyrolysis. The aqueous solution of zinc acetate, ammonium acetate and different indium sources: indium (III) chloride and indium (III) nitrate were used as the precursors. After film deposition, different anneal temperature treatment as 350, 450, 550^{o}C were applied. Electrical properties as concentration and mobility were characterized by Hall measurement. The surface morphology and crystalline quality were characterized by SEM and XRD. With the activation energy analysis for both films, the concentration variation of the films at different heat treatment temperature was realized. Donors correspond to zinc related states dominate the conduction mechanism for these INZO films after 550 ^{o}C high temperature heat treatment process.

Keywords: indium-nitrogen co-doped zinc oxide; anneal; resistivity

1. Introduction

Zinc oxide (ZnO) thin film has been used widely for recent decades. In the device applications, ZnO has been the limelight since it is generally used in solar cells (Yuan *et al*. 2006), piezoelectric devices (Wang *et al*. 2006), transparent electrodes (Yamamoto *et al*. 2012), gas sensor (Mitra *et al*. 1998) etc.. To obtain the ZnO film, lots of techniques can be used, such as ion beam deposition (Yuan *et al*. 2006), sputtering (Wang *et al*. 2006, Yamamoto *et al*. 2012), chemical vapour deposition CVD (Mitra *et al*. 1998), spray pyrolysis SP (Studenikin *et al*. 1998), sol-gel (Tsay and Wang 2013), pulsed laser deposition (PLD) (Mendelsberg *et al*. 2008) et cetera. Compared with other deposition method, the spray pyrolysis method is one of the attractive technique with the advantage of easy scale up (Paraguay *et al*. 1999, DocumentIslam and Podder 2009), high deposition rate and without high-vacuum equipment (Singh *et al*. 2007, Du *et al*. 2006).

Different precursor species (DocumentKang *et al*. 2000, Skrabalak and Suslick 2006, Dunkle *et al*. 2009) can be applied in the spray pyrolysis technology. Less discussion about comparison the ZnO films with different precursor by spray pyrolysis. As co-doped skill for the semiconductor

*Corresponding author, Professor , E-mail: ocean@ntut.edu.tw

http://www.techno-press.com/?journal=anr&subpage=7 ISSN: 2287-237X (Print), 2287-2388 (Online)

(Fan *et al*. 2013, Yamamoto and Yoshi 2001) shows the ability of stable and low resistive results. Thus, indium and nitrogen co-doped ZnO were prepared by spray pyrolysis technology with different indium precursors: indium (III) chloride (ZIC) and indium (III) nitrate (ZIN) in this paper. The film morphology, crystalline quality and conducting properties were studied.

2. Experimental details

The indium and nitrogen co-doped ZnO (n-ZnO) thin film with undoped ZnO interlayer was deposited on glass substrate at 475^{o}C. The undoped ZnO interlayer was formed from the pyrolysis of the precursor of zinc chloride aqueous solution 0.2 M. And the n-ZnO film was formed from the pyrolysis of the precursor of zinc acetate, ammonium acetate and different indium sources: indium (III) chloride and indium (III) nitrate with ratio 1:3:0.05. (Fan *et al*. 20113) The prepared solution was hen sprayed on the heated glass substrates by ultrasonic spray pyrolysis. After deposition, samples were then cut to separate pieces and one was named as as-grown sample, the others was then proceeded with different high temperature treatment in atmosphere as 350, 450, 550^{o}C for 20minutes. The In contact was formed by soldering followed by 350^{o}C annealing process for 5 minutes.

A scanning electron microscopy (SEM, Hitachi S-300H) was used to characterize the surface morphology. The crystalline structure was obtained by x-ray diffractometry (XRD, Bruker D8). The conductivity was obtained by van der Pauw four-point method (KEITHLEY 2400) and carrier concentration and mobility were obtained by Hall measurement with magnetic field strength 0.42 T.

3. Results and discussion

Fig. 1 and Fig. 2 shows the surface morphology characterized by SEM for the ZIN and ZIC films, respectively. To ZIC film, after the anneal process, the nanosized particals on the surface

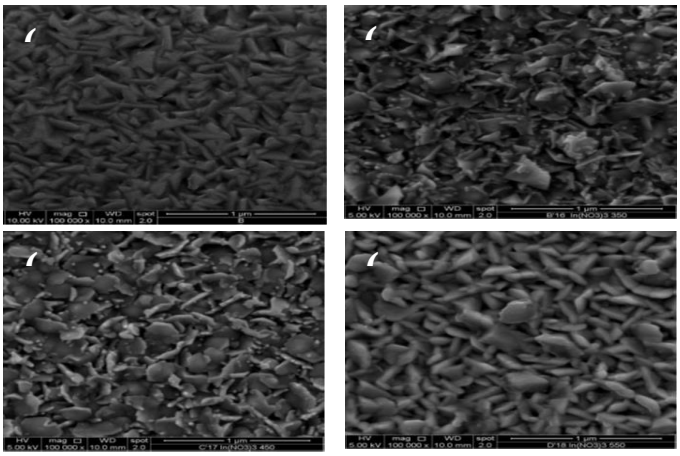

Fig. 1 the surface morphology characterized by SEM for the ZIN (a) as grown and after heat treatment at temperatures, (b) 350 ^{o}C, (c) 450 ^{o}C (d) 550 ^{o}C

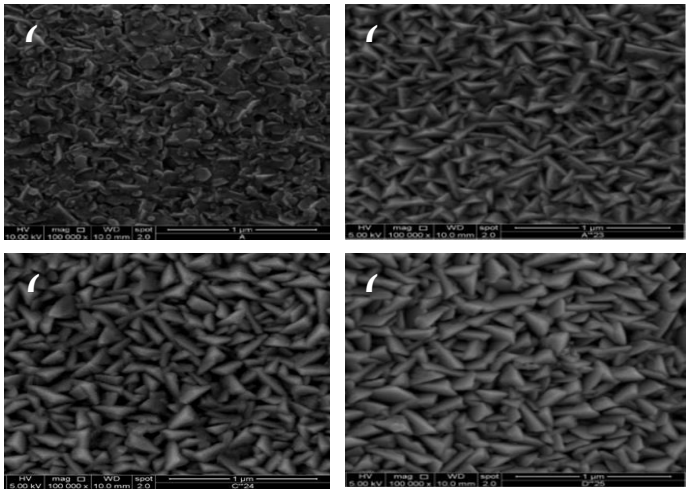

Fig. 2 the surface morphology characterized by SEM for the ZIC films (a) as grown and after heat treatment at temperatures, (b) 350 °C, (c) 450 °C and (d) 550 °C

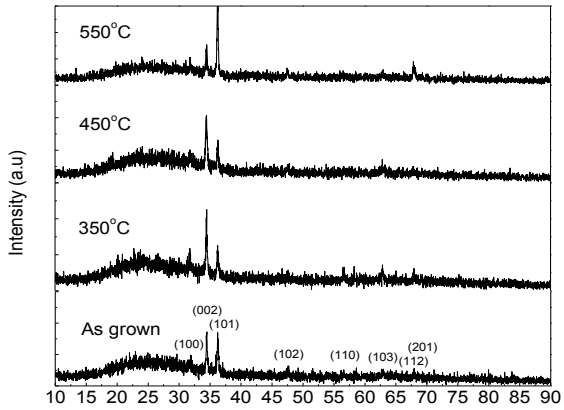

Fig. 3 shows the XRD spectrum of the ZIN film after heat treatment at different temperatures

clearly changes, from petal-like turn into cube-like. For ZIN film, the anneal process influences the film morphology also. With higher temperature, leaf-like morphology can be observed. As the temperature reach 550°C, mixed leaf-like and cube-like morphology can be observed. With the annealing temperature rising up, both samples show that the surface morphology varies and larger grain can be characterized.

Fig. 3 shows the XRD spectrum of the ZIN film annealed at different temperatures. The as grown ZIN films shows obvious (002) and (101) peaks. Some weak signal such as (100), (102), (103) and (112) can be observed also. The two main peaks (002) and (101) both remains as the heat treatment temperature reaches to 550 °C.

Fig. 4 shows the XRD spectrum of the ZIC films annealed at different temperatures. It was found that main peaks correspond to ZnO (002) and (101) structure can be observed for the as grown film. Furthermore, some weak peak corresponded to (102) and (112) can be observed also.

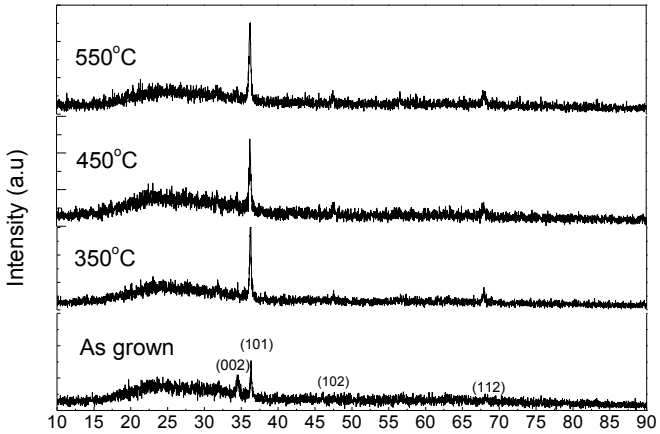

Fig. 4 shows the XRD spectrum of the ZIC film after heat treatment at different temperatures

The (002) peak decreases and (101) peak increases as the temperature increases. The (101) peak becomes the dominate peak for these annealed samples.

The carrier concentration and mobility for ZIN and ZIC samples with different heat treatment temperature were shown in Table I and Table II, respectively. All the films exhibited n-type conductivity. For ZIN film, the concentration decreases from 1.2×10^{20} cm^{-3} to 3.1×10^{17} cm^{-3} as the heat treatment temperature increases to 450 °C. The concentration increases to 2.9×10^{19} cm^{-3} as the temperature reaches 550°C. Such concentration increasing may be corresponded to donor species occurring in the film. The mobility shows an increasing behavior as the heat treatment temperature increases to 450°C. As the heat treatment is beneficial for better crystal quality and larger grain can be observed in Fig. 1, less electron scattering and the increasing of mobility can be expected in this region. As the temperature increase to 550°C, the decrease of mobility may be corresponded to extra introduce of carriers as characterized in the concentration measurement.

For ZIC film, as shown in Table II, the concentration decreases from 3.1×10^{19} cm^{-3} to 2.0×10^{18} cm^{-3} as the heat treatment temperature increases to 450°C. The concentration increases to 5.8×10^{19} cm^{-3} as the temperature reaches 550°C. Similar concentration increasing as ZIN film can be observed. The carrier mobility decreases the temperature increases to 550°C.

To better understand the origin of electrical conduction, temperature dependent film conductivity measurement was carried out. Fig. 5 shows the conductivity of the ZIN films plotted as functions of inverse measurement temperature. The relationship between conductivity σ and the measurement temperature T is given by Yamamoto and Yoshid (2001)

$$\sigma = \sigma_0 \exp(-E_A / kT) \tag{1}$$

where σ_0 is the pre-exponential factor, k is the Boltzmann constant, EA is the activation energy. The calculated EA values were listed in Table I and II.

Fig. 5 shows the temperature dependence of electrical conductance for the ZIN film after different heat treatment temperature. For the as grown ZIN film, as shown in Table I, the obtained activation energy is 24 meV. This activation value, which is near 26 meV, is corresponded to the origin donor level for the indium doped ZnO (Ye *et al.* 2007). While the heat treatment temperature increases to 450°C, the conductivity decrease and two linear regions corresponding to

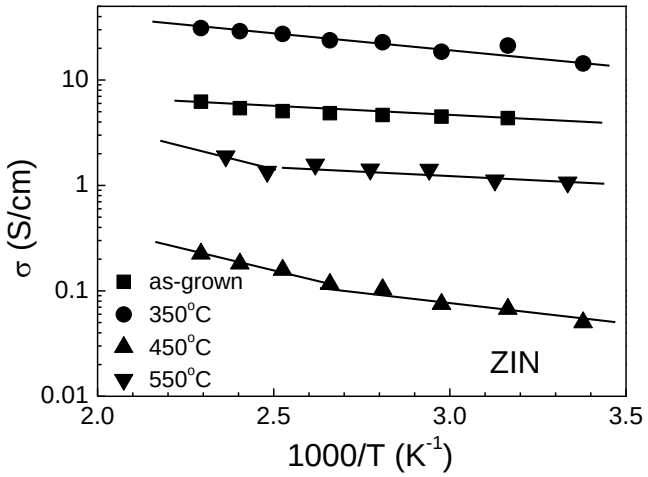

Fig. 5 Temperature dependence of electrical conductance for the ZIN film after different heat treatment temperatures

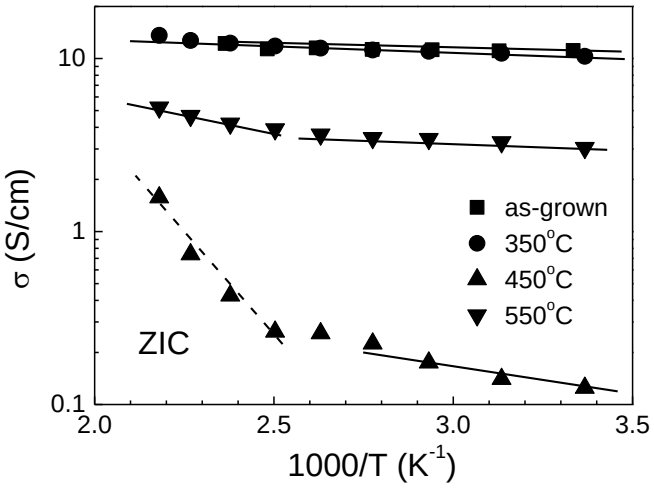

Fig. 6 Temperature dependence of electrical conductance for the ZIC film after different heat treatment temperatures

different measurement temperature range can be observed in the figure. The extracted activation energy 80 meV, which is the octahedral zinc interstitial (Zni^{2+}) (Benhaliliba *et al*. 2010), and 162 meV, as zinc vacancy (V_{Zn}) (Ilican *et al*. 2006) can be observed in many ZnO films. While the heat treatment temperature increase to 550°C, two temperature regions remains and two activation energy values can be obtained. The activation energy is 35 meV may correspond to zinc atoms in tetrahedral positions (Benhaliliba *et al*. 2010, Kumar *et al*. 2005) or the charged zinc interstitials (Pagni *et al*. 2006). And the higher activation energy 157 meV may correspond to higher charged zinc vacancy transition (V_{Zn}) (Ilican *et al.* 2006, Pagni *et al*. 2006).

Fig. 6 shows the temperature dependence of electrical conductance for the ZIC film after different heat treatment temperature. The samples without annealing treatment and with the heat

treatment at 350^{o}C both have the shallow donor level.The activation energies may be both denoted by interstitial zinc (Zni^{+}) (Fang and Farlow 2007, Sun and Wang 2003, Lee *et al*. 2010). The activation energy shows two values as the heat treatment temperature increases to 450^{o}C. The one is 84 meV, named octahedral zinc interstitials (Zni^{2+}) (Benhaliliba *et al*. 2010), and the other is 455 meV, caused by grain boundary sacttering (Ye *et al*. 2007). As the heat treatment temperature increase to 550^{o}C, two activation energy values can be obtained. The activation energy 22 meV is corresponded to the shallow donor state (Ye *et al*. 2007, Fang and Farlow 2007). The other activation energy 82 meV may correspond to vacancy-related state octahedral zinc interstitials. (Benhaliliba *et al*. 2010, Ilican *et al*. 2006).

For ZIN film, as the heat treatment temperature increases to 450^{o}C, the concentration decreases as the reduction of origin shallow donor. And some zinc vacancy may arose while the temperature at 450^{o}C. As the temperature reaches 550^{o}C, this Zn vacancy remains and some certain donor state associated with Zn in tetrahedral position causes the increasing in concentration at room temperature. For ZIC film, shallow donors with smaller activation energy value can be observed for the as grown film. The concentration decreases coming from the reduction of the shallow donors can be observed also as the heat treatment temperature increases to 450^{o}C. Carrier concentration increasing again as the heat treatment temperature increases from 450 to 550^{o}C by the creation of some certain zinc-related vacancy and charged states.

4. Conclusions

Indium-nitrogen co-doped ZnO (INZO) films were prepared on glass substrate by ultrasonic spray pyrolysis (USP). It is found that ZIN film, using indium (III) nitrate as precursor, shows obvious two main peaks (002) and (101). Both two peaks remain as the heat treatment temperature reaches to 550^{o}C. For ZIC film, using indium (III) chloride as precursor, the preferred peak (101) increases clearly as the heat temperature increase. Two films are both Polycrystalline patterns. Characterized from scanning electron microscopy (SEM), the film with different precursor would cause different surface morphology. The conducting properties of INZO films influence by defect states significantly. Different defects and types are caused by different precursors and heat treatment temperatures. After 550^{o}C high temperature treatment, shallow donors correspond to different zinc related states dominate the conduction mechanism at room temperature for both films.

Acknowledgments

Financial support of this paper was provided by the Ministration of Science and Technology of the Republic of China under Contract no. MOST 103-2221-E-027-029-MY2.

References

Benhaliliba, M.C., Benouis, E., Aida, M.S., Yakuphanoglu, F. and Juarez, A.S. (2010), "Indium and aluminium-doped ZnO thin films deposited onto FTO substrates: nanostructure, optical, photoluminescence and electrical properties", *J. Sol-Gel. Sci. Technol.*, **55**, 335-342.

DocumentKang, Y.C., Lenggoro, I.W., Park, S.B. and Okuyama, K. (2000), "YAG:Ce phosphor particles prepared by ultrasonic spray pyrolysis", *Mater. Res. Bul.*, **35**(5), 789-798.
DocumentIslam, M.R. and Podder, J. (2009), "Optical properties of ZnO nano fiber thin films grown by spray pyrolysis of zinc acetate precursor", *Cryst. Res. Tech.*, **44**(3), 286-292.
Du, G.T., Liu, W.F., Bian, J.M., Hu, L.Z., Liang, H.W., Wang, X.S., Liu, A.M. and Yang, T.P. (2006), "Room temperature defect related electroluminescence from ZnO homojunctions grown by ultrasonic spray pyrolysis", *Appl. Phys. Lett.*, **89**(5), 052113.
Dunkle, S.S., Helmich, R.J. and Suslick, K.S. (2009), "BiVO4 as a visible-light photocatalyst prepared by ultrasonic spray pyrolysis", *J. Phys. Chem. C*, **113**(28), 11980-11983.
Fan, J.C., Sreekanth, K.M., Xie, Z., Chang, S.L. and Rao, K.V. (2013), "p-Type ZnO materials: Theory, growth, properties and devices", *Prog. Mater. Sci.*, **58**(6), 874-985.
Fang, Z.Q. and Farlow, G.C. (2007), "Electron irradiation induced deep centers in hydrothermally grown ZnO", *J. Appl. Phys.*, **101**, 086106.
Gür, E., Tüzemen, S. and Dogan, S. (2009), "Temperature-dependent electrical characterization of nitrogen-doped ZnO thin film: vacuum annealing effect", *Physica Scripta*, **79**, 035701-1-5.
Ilican, S., Caglar, Y., Caglar, M. and Yakuphanoglu, F. (2006), "Electrical conductivity, optical and structural properties of indium-doped ZnO nanofiber thin film deposited by spray pyrolysis method", *Physica E*, **35**, 131-138.
Kumar, P.M.R., Kartha, C.S., Vijayakumar, K.P., Singh, F. and Avasthi, D.K. (2005), "Effect of fluorine doping on structural, electrical and optical properties of ZnO thin films", *Mater. Sci. Eng. B*, **117**, 307-312.
Lee, H.Y., Xia, S.D., Zhang, W.P., Lou, L.R. and Yan, J.T. (2010), "Mechanisms of high quality i-ZnO thin films deposition at low temperature by vapor cooling condensation technique", *J. Appl. Phys.*, **108**, 073119.
Mende, L.S. and MacManus-Driscoll, J.L. (2007), "ZnO-nanostructures, defects, and devices", *Materialst.*, **10**(5), 40-48.
Mendelsberg, R.J., Kerler, M., Durbin, S.M. and Reeves, R.J. (2008), "Photoluminescence behavior of ZnO nanorods produced by eclipse PLD from a Zn metal target", *Superlat. Microstr.*, **43**, 594-599.
Mitra, P., Chatterjee, A.P. and Maiti, H. S. (1998), "Chemical deposition of ZnO films for gas sensors", *J. Mater. Sci., Mater. Elect.*, **9**, 441-445.
Pagni, O., Somhlahlo, N.N., Weichsel, C. and Leitch, A.W.R. (2006),"Electrical properties of ZnO thin films grown by MOCVD", *Physica B*, **376-377**, 749-751.
Paraguay, D.F., Estrada, L.W., Acosta, N.D.R., Andrade, E. and Miki-Yoshida, M. (1999), "Growth, structure and optical characterization of high quality ZnO thin films obtained by spray pyrolysis", *Thin Solid Film.*, **350**(1), 192-202.
Singh, P., Kumar, A., Deepak. and Kaur, D. (2007), "Growth and characterization of ZnO nanocrystalline thin films and nanopowder via low-cost ultrasonic spray pyrolysis", *J. Cryst. Growth*, **306**(2), 303-310.
Skrabalak, S.E., Suslick, K.S. (2006), "Porous carbon powders prepared by ultrasonic spray pyrolysis", *J. Am. Chem. Soc.*, **128**(39), 12642-12643.
Studenikin, S. A., Golego, N. and Cociverab, M. (1998), "Density of band-gap traps in polycrystalline films from photoconductivity transients using an improved Laplace transform method", *J. Appl. Phys.*, **84**(9), 5001-5004.
Sun, Y. and Wang, H. (2003), "The electronic properties of native interstitials in ZnO", *Physica B*, **325**, 157-163.
Tsay, C.Y. and Wang, M.C. (2013), "Structural and optical studies on sol-gel derived ZnO thin films by excimer laser annealing", *Ceram. Int.*, **39**, 469-474.
Wang, X.B., Song, C., Li, D.M., Geng, K.W., Zeng, F. and Pan, F. (2006), "The influence of different doping elements on microstructure, piezoelectric coefficient and resistivity of sputtered ZnO film", *Appl. Surf. Sci.*, **253**, 1639-1643.
Yamamoto, N., Makino, H., Osone, S., Ujihara, A., Ito, T., Hokari, H., Maruyama, T. and Yamamoto T. (2012), "Development of Ga-doped ZnO transparent electrodes for liquid crystal display panels", *Thin*

Solid Film., **520**, 4131-4138.
Yamamoto, T. and Yoshid, H.K. (2001), "Physics and control of valence states in ZnO by codoping method", *Physica B*, **302-303**, 155-162.
Ye, H.B., Kong. J.F., Shen, W.Z., Zhao, J.L. and Li, X.M. (2007), "Origins of shallow level and hole mobility in codoped p-type ZnO thin films", *Appl. Phys. Lett*., **90**, 102115.
Yuan, N., Li, J., Fan, L., Wang, X. and Zhou, Y.(2006), "Structure, electrical and optical properties of N-In codoped ZnO thin films prepared by ion-beam enhanced deposition method", *J. Cryst. Growth*, **290**, 156-160.

CC